Experimental Validation of the Linear Theory of Stimulated Raman Scattering Driven by a 500-fs Laser Pulse in a Preformed Underdense Plasma

C. Rousseaux, G. Malka, and J. L. Miquel
Commissariat à l'Energie Atomique, Centre d'Etudes de Limeil-Valenton, 94195 Villeneuve-St-Georges Cedex, France

F. Amiranoff and S. D. Baton
Laboratoire pour l'Utilisation des Lasers Intenses, Ecole Polytechnique, 91128 Palaiseau Cedex, France

Ph. Mounaix
Centre de Physique Théorique, Ecole Polytechnique, 91128 Palaiseau Cedex, France
(Received 7 June 1994)

Measurements of stimulated Raman scattering (SRS) reflectivity produced by the interaction between a short 450-fs, 1.06-μm laser pulse and a large underdense preformed plasma are presented. Experimental results show that the SRS reflectivity sharply increases as the intensity of the interaction beam approaches 10^{16} W/cm^2 from below and saturates for intensities greater than 10^{17} W/cm^2. These results are found to be in very good agreement with those of the initial transient stage theory of SRS starting from thermal equilibrium noise.

PACS numbers: 52.40.Nk, 42.65.Dr, 52.35.Mw

Stimulated Raman scattering (SRS) in the backward direction is a parametric instability in which an incident electromagnetic wave (EMW) resonantly decays into a backscattered electromagnetic wave and an electron plasma wave (EPW) [1–3]. This instability is an important issue in the context of laser inertial confinement fusion (ICF) and gas-target experiments using femtosecond lasers. In both cases it can lead to scattering and redistribution of the incident light energy and may reduce the efficiencies of fs-laser applications such as x-ray laser [4], wake-field generation [5], or high harmonics generation [6]. In previous works [7], it has been shown that for long laser pulses ($\sim$1 ns) the backward SRS reflectivity correctly follows the predictions of a convective gain model provided that the onset of absolute instability is prevented by using smoothed laser beam. On the other hand, in the absence of beam smoothing and in the case of sufficiently intense and long laser pulses, SRS is absolute and has enough time to reach a highly nonlinear saturated state. Thus, above the absolute threshold, a comparison between experiments and the linear theory of the instability is possible only in the case of very short pulses (e.g., with durations typically shorter than the characteristic time of the onset of absolute instability behavior). So far, the amount of experimental data on SRS with short pulses that has been published has only been devoted to the interactions between high intensity short laser pulses and gases, either gas jet targets [8] or static fills of gas [9,10]. In these experiments, the gas was not fully ionized, with a very low electron density (typically $n/n_c \leq 10^{-3}$), and the SRS reflectivity was always very weak, 10^{-4} in the most favorable conditions of pressure, gas species, and intensity of the pump laser [9].

In this Letter, we report experimental observations of SRS in the backward direction produced by the interaction between a subpicosecond laser pulse, without beam smoothing, and a large underdense preformed plasma. This work complements the earlier studies on SRS with beam smoothing by using a different mechanism (short pulse length) to simplify the SRS interaction and deal with much higher intensities. The main result shows that the SRS reflectivity sharply increases from below 10^{-7} up to a few tens of percents as the intensity of the interaction beam is raised from 5×10^{15} to 10^{17} W/cm^2. It then saturates for intensities between 10^{17} and 10^{18} W/cm^2. These results have been compared with the predictions of the linear theory of SRS assuming that the instability grows from *thermal* noise.

The experiment was performed at CEA, Centre d'Etudes de Limeil-Valenton (CEL-V) using the P102 laser facility. This laser generates up to 50-TW power pulses centered at 1.058 μm wavelength by using the chirped-pulse-amplification technique applied to a Ti:sapphire/Nd:silicate power chain [11]. For our experiment, the chirped initial laser beam was split into two different beams (Fig. 1): The first one was used to preform the plasma while the second one interacted with the underdense preformed plasma after being temporally compressed by a pair of gratings. This configuration allows one to study the interaction over a large range of laser intensity with the same plasma conditions.

The first beam, the creation beam, had a duration of 500 ps full width at half maximum (FWHM); it was focused by a $f/8$ lens in a direction perpendicular to the target plane onto a thin plastic foil (CH). After being frequency doubled by using a potassium dihydrogen phosphate (KDP) crystal (associated to a BG18 filter to suppress

0031-9007/95/74(23)/4655(4)$06.00

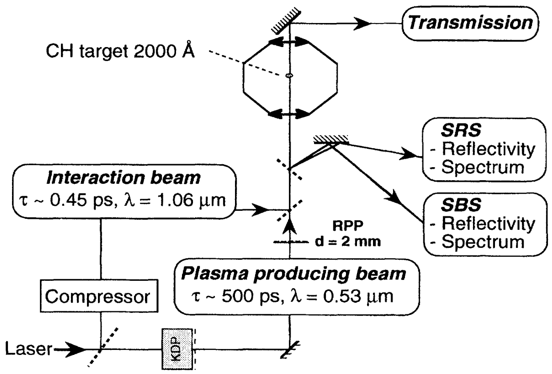

FIG. 1. Experimental setup.

the residual infrared light), the spectrum of this chirped beam had a central wavelength of 0.529 μm. A random phase plate (RPP) with 2 mm $\times$ 2 mm elementary cells was added to improve the reproducibility of the plasma conditions shot by shot. The intensity of the creation beam on target was maintained at 4×10^{12} W/cm^2, corresponding to an energy of 2.5 J contained in the 400 μm focal spot diameter. The target thickness (200 nm) and the time delay between the two beams ($\Delta t = 1.7$ ns) were chosen so as to obtain a subtenth critical plasma density for the whole duration of the interaction [12,13]. The density and the temperature profiles, as well as the ionization state, were estimated from one-dimensional (1D) hydrodynamic simulations CHIVAS [14]. Just before the arrival of the interaction beam we obtained a fully ionized plasma characterized by a 1 mm FWHM Gaussian electron density profile with a maximum of $0.07n_c$ and an electron temperature of about 100 eV.

The second beam, the interaction beam, was focused collinearly with the first beam by the same $f/8$ lens onto a smaller focal spot of 40 μm in diameter which corresponds to 90% of the incident energy. Images of the focal spot showed a smooth intensity profile without significant hot spots. The spectrum of this beam was centered at 1.058 μm with a spectral width of about 5 nm FWHM. The pulse duration, routinely measured at each shot by a single-shot autocorrelator, was typically 450 fs FWHM. The energy of the interaction beam on target was varied from 30 mJ to 7 J by locating optical-quality attenuators in the beam path before the pair of gratings. A pedestal of 1 ns duration preceded the main pulse; the peak-to-background intensity contrast ratio was measured to be better than 10^5:1.

The backscattered light was collected through the focusing lens of aperture $\Delta\Omega = 0.02$ sr, which imaged the plasma to different diagnostics in order to simultaneously obtain SRS spectrum and energy. Namely, the SRS light was analyzed by a spectrometer associated with an InGaAs detector permitting the recording of spectra up to 1.6 μm. The SRS energy was measured by a fast InGaAs photodiode (300 ps rise time) with a nearly constant spectral response between 1.1 and 1.6 μm. Reflectivity at wavelengths near the fundamental wavelength (1.058 μm) was systematically suppressed by means of filters that attenuated the 1 μm light by a factor greater than 10^6. The transmitted light was imaged through a $f/8$ lens onto a fast S1 photodiode. An other fast S1 photodiode was used to measure the stimulated Brillouin scattering (SBS) reflectivity. In the latter diagnostic, the very low sensitivity of the S1 photodiode for wavelengths greater than 1.1 μm insured the contribution of the parasitic light coming from SRS to be negligible. Increasing the laser intensity from 3×10^{14} to 10^{18} W/cm^2, we found that the energy transmission rate varies from a few percents to 20% and that the SBS reflectivity varies from 10^{-6} to 10^{-1}. In the following, we present and discuss only results concerning the SRS spectra and the time integrated SRS reflectivity as a function of the laser intensity.

Figure 2 shows time integrated typical spectra of the SRS backscattered light at two different laser intensities. For both low intensity [Fig. 2(a), $I = 10^{16}$ W/cm^2] and high intensity [Fig. 2(b), $I = 4 \times 10^{17}$ W/cm^2] the spectra of the backscattered light were centered at a wavelength close to 1.46 μm. According to the usual three wave resonance conditions for SRS, one finds that this value corresponds to an electron plasma density of $0.07n_c$ in agreement with the 1D hydrodynamic simulations [14]. The width (FWHM) of the spectra was observed to increase with the laser intensity, typically from about 20 nm at 2×10^{16} W/cm^2 to 60 nm at 6×10^{17} W/cm^2. It has been seen that at high intensities [e.g., Fig. 2(b)] the spectra displayed strong modulations typically spaced by 15 nm, contrary to spectra at low intensities. We did not find any simple interpretation for these modulations.

The squares in Fig. 3 represent the experimental SRS reflectivity as a function of the laser intensity. This reflectivity is the ratio of the SRS energy backscattered through the focusing lens to the incident laser energy. The shaded area corresponds to a backscattered energy less than 3×10^{-10} J which is the detection threshold of the diagnostic device. The points with vertical error bars

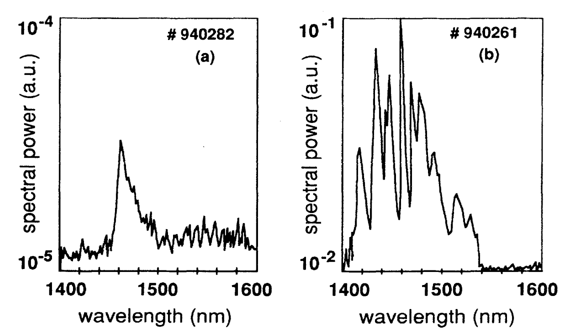

FIG. 2. SRS spectra at two different laser intensities: (a) $I = 10^{16}$ W/cm^2 and (b) $I = 4 \times 10^{17}$ W/cm^2.

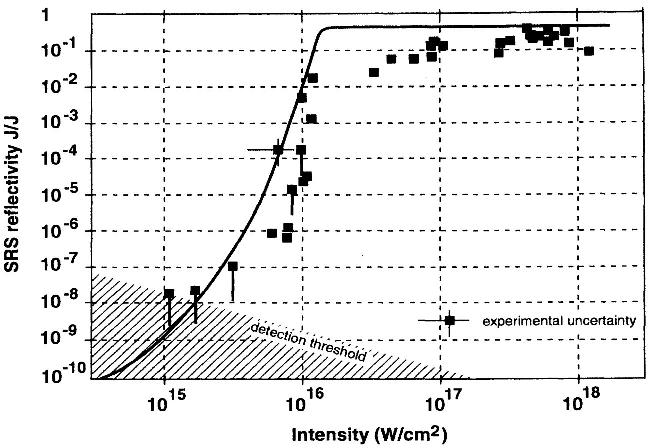

FIG. 3. Time integrated SRS reflectivity as a function of the laser intensity for $n/n_c = 0.07$, $T_e = 0.1$ keV, and $L = 600$ μm. The squares are the experimental data, and the solid line is the theoretical curve as given by Eq. (1). The shaded area corresponds to a backscattered energy less than the detection threshold. The experimental uncertainty displayed as a footnote is systematic and is to be applied to each experimental point.

correspond to an overestimated value of the reflectivity when the signal is very weak or null. The typical experimental uncertainty of our measurements essentially originates from the actual value of the laser intensity in the plasma and from the calibration of the detector system in the 1.2 to 1.6 μm range. One can see the following: (i) the SRS reflectivity increases very sharply from below 10^{-7} to a few percent for incident laser intensities rising from 3×10^{15} to 10^{16} W/cm^2; and (ii) the reflectivity saturates at a few tens of percent for intensities between 10^{17} and 10^{18} W/cm^2.

Measurements of SRS reflectivity as displayed in Fig. 3 strongly suggest that the SRS *nonlinear* saturation only starts playing a significant role for pump intensities above 2×10^{16} W/cm^2. It follows that for lower intensities the reflectivity is expected to be analytically obtained from theoretical estimates based upon the *linear* theory of SRS. The theoretical model we used has already been extensively described in Ref. [15]. For the reader's convenience we summarize here the principal points that characterize this model: (i) A 1D model is used in which the waves propagate in an underdense homogeneous plasma of finite length L. (ii) The incident pulse of peak intensity $I_{\max}$ and characteristic duration t_p is replaced by a square pulse of intensity I_0 and duration t_p, where I_0 is determined so that the total energy is identical to the incident energy. (iii) The parametric growth is solved in terms of fluctuating initial and boundary conditions corresponding to thermal noise at equilibrium. Fluctuating source terms, representing thermal noise emission of waves, are accordingly retained in the coupled mode equations.

The problem of the time evolution of the reflectivity as given by this theory is out of the scope of this paper, and we will restrict ourselves to the time integrated reflectivity to be compared with the experimental results of Fig. 3. For pulse duration such that $t_p < (4L/c)(1 - n/n_c)^{-1/2}$, which is always satisfied in our experimental conditions, one finds that the linear time integrated SRS reflectivity is given by

$$R_L \approx (2\pi)^2\left(\frac{\Sigma_2^{1\mathrm{D}}}{2\nu_2}\right)\frac{\gamma}{2^{3/2}c\sqrt{1-n/n_c}}\left[\frac{1}{2\gamma t_p}+\frac{2L}{ct_p\sqrt{1-n/n_c}}-\frac{1}{2}+\frac{\sqrt{\pi}}{2\sqrt{\gamma t_p}}\right]\frac{\exp(2\gamma t_p)}{\sqrt{2\pi\gamma t_p}}, \tag{1}$$

with $\gamma = \gamma_0/\sqrt{2}$ where

$$\frac{\gamma_0}{\mathrm{ps}^{-1}} = 4.03\frac{(n/n_c)^{1/4}(I_{14}\,\lambda_0^2)^{1/2}[(1-n/n_c)^{1/2}+(1-2\sqrt{n/n_c})^{1/2}]}{\lambda_0(1-n/n_c)^{1/4}(1-\sqrt{n/n_c})^{1/2}}$$

is the homogeneous SRS growth rate; here λ_0 denotes the vacuum laser wavelength in μm and $I_{14}\,\lambda_0^2$ is the vacuum laser flux in units of 10^{14} W cm^{-2} μm^{-2}. The validity condition for Eq. (1) corresponds to that of the so-called standard decay regime where the envelope approximation is valid for each of the interacting waves. It reads

$$I_{14}\,\lambda_0^2 < 3.64\times10^5(n/n_c)^{1/2}\frac{1-(n/n_c)^{1/2}}{\{(1-n/n_c)^{1/2}+[1-2(n/n_c)^{1/2}]^{1/2}\}^2}. \tag{2}$$

The quantity $\Sigma_2^{1\mathrm{D}}/2\nu_2$ appearing in expression (1) is proportional to the EPW spectral density at the wave number corresponding to the usual three wave resonance conditions for SRS. At thermal equilibrium, this quantity reads

$$\frac{\Sigma_2^{1\mathrm{D}}/2\nu_2}{1\ \mu\mathrm{m}} = 3.1\times10^{-10}\frac{(1-n/n_c)^{1/2}[(1-n/n_c)^{1/2}+(1-2\sqrt{n/n_c})^{1/2}]^2}{(n/n_c)^{1/2}}\frac{T_e}{1\ \mathrm{keV}}\frac{\Delta\Omega}{I_{14}\,\lambda_0^2}, \tag{3}$$

where the solid angle $\Delta\Omega = 0.02$ sr corresponds to the aperture of the collected lens.

In the regimes where the reflectivity is no longer small compared to unity, it is necessary to take into account both the pump depletion and the coupling between SRS EPW and the ion acoustic waves (IAW). In the limit of a 1D model it has been observed numerically [16,17] that for time scales as short as 0.5 ps the coupling between EPW and IAW has no time to play an important role as far as the backward SRS reflectivity is concerned. On the other hand, it can be shown from the Manley-Rowe relations properly modified to take into account the laser pulse propagation [15] that, in the linear stage of the instability, the ratio of the SRS EPW energy to that of the backscattered transverse wave is equal to $2\sqrt{n/n_c}/(1 - \sqrt{n/n_c})$. Assuming then that, at saturation, all the available incident energy is totally dispatched between the two SRS daughter waves, one finds that the energy of the backscattered transverse wave must be less than $R_{\max} \equiv \eta(1 - \sqrt{n/n_c})/(1 + \sqrt{n/n_c})$, where the factor η denotes the fraction of the incident energy which is available for backward SRS. Accordingly, we will roughly take into account the pump depletion by approximating the time integrated SRS reflectivity R by

$$1/R \approx 1/R_L + 1/R_{\max}, \tag{4}$$

where the linear reflectivity R_L is given by Eq. (1).

We have checked that R does not depend strongly on the electron temperature and density; for this reason we will make the comparison between theoretical predictions and experimental data by choosing the most typical values for the physical parameters, namely, $T_e = 0.1$ keV and $n/n_c = 0.07$. Note that in this limit condition (2) reads $I_{14}\,\lambda_0^2 < 2 \times 10^4$, which is always satisfied in the laser intensity domain of interest. The remaining parameters are $Z = 5.3$, $A = 6.5$, and $\lambda_0 = 1.058\ \mu$m. For these parameters, we have also checked that at low intensities ($<10^{16}$ W/cm^2) the pedestal intensity is always below the SRS homogeneous collisional threshold. At high intensities ($>10^{16}$ W/cm^2) the SRS reflectivity nonlinearly saturates (cf., Fig. 3), and considering possible effects of the pedestal is no longer relevant.

Figure 3 shows the theoretical curve as given by Eq. (4) for an interaction length $L = 600\ \mu$m corresponding to the Rayleigh length of the focusing optics; the squares represent the experimental data. The factor η appearing in the expression for $R_{\max}$ has been assumed to be given by $\eta \approx 1 - T - R_{\rm SBS}$, where $T \approx 0.2$ and $R_{\rm SBS} \approx 0.1$ are, respectively, the measured energy transmission rate and the measured backward SBS time integrated reflectivity in the large flux regime $I_{14}\,\lambda_0^2 > 2 \times 10^2$. We have therefore neglected both SRS and SBS sidescattering as well as the absorption of EMW. It can be seen that the theoretical reflectivity (4) is in very good agreement with that experimental results. This leads to the two following remarks.

(i) In the linear regime of the instability ($2 \times 10^1 < I_{14}\lambda_0^2 < 2 \times 10^2$), SRS reflectivity proves to be properly described by the standard three wave theory in which the instability grows from *thermal equilibrium* noise [15]. In this regime, one can attribute the slight overestimation of the experimental data by the theoretical curve to our neglecting SRS side scattering and/or to a slight underestimation of the actual local laser intensity due to the inhomogeneity of the focal spot.

(ii) In the large flux regime ($I_{14}\,\lambda_0^2 > 10^3$), the theoretical estimate $R \approx R_{\max}$ is found to slightly overestimate the actual reflectivity. This result is expected and can be attributed to our neglecting different effects, such as SBS and SRS sidescattering and/or EMW absorption that tend to lessen the value of $R_{\max}$ by diminishing that of η.

It is worth noting that these results are strikingly different from those of similar short pulse experiments devoted to stimulated Brillouin scattering [18,19]. Indeed, in the latter case a large discrepancy has always been found between theoretical predictions of SBS from *thermal* noise and experimental results.

In summary, we have observed stimulated Raman scattering produced by the interaction between an intense subpicosecond laser pulse and a large underdense preformed plasma. The main result shows very good agreement between experiment and theory for time integrated reflectivity. Such an agreement leads to the conclusion that short pulse driven SRS can properly be described by the linear theory of three wave parametric instabilities growing from *thermal equilibrium* noise.

We would like to thank C. Chenais-Popovics, J. C. Gauthier, P. Mora, D. Pesme, and W. Rozmus for fruitful discussions. We also wish to acknowledge encouragement and support from M. Decroisette and J. Coutant as well as the technical assistance of the P102-Castor staff at CEA Limeil. We are particularly grateful to I. Allais, A. Pierre, and C. Rouyer for their help and skill during this experiment.

[1] C. S. Liu, M. N. Rosenbluth, and R. B. White, Phys. Fluids **17**, 1211 (1974).
[2] J. F. Drake *et al.*, Phys. Fluids **17**, 778 (1974).
[3] D. W. Forslund, J. M. Kindel, and E. L. Lindman, Phys. Fluids **18**, 1002 (1975).
[4] N. H. Burnett and P. B. Corkum, J. Opt. Soc. Am. B **6**, 1195 (1989).
[5] T. Tajima and J. M. Dawson, Phys. Rev. Lett. **43**, 267 (1979).
[6] A. L'Huillier, Ph. Balcou, and L. A. Lompré, Phys. Rev. Lett. **68**, 166 (1992).
[7] S. P. Obenschain *et al.*, Phys. Rev. Lett. **62**, 768 (1989).
[8] M. Dunne *et al.*, Phys. Rev. Lett. **72**, 1024 (1994).
[9] Z. Najmudin *et al.*, (private communication).
[10] C. B. Darrow *et al.*, Phys. Rev. Lett. **69**, 442 (1992).
[11] C. Rouyer *et al.*, Opt. Lett. **18**, 214 (1993).
[12] R. Fabbro *et al.*, Phys. Rev. A **26**, 2289 (1982).
[13] R. A. London and M. D. Rosen, Phys. Fluids **29**, 3813 (1986).
[14] S. Jacquemot and A. Decoster, Laser Part. Beams **9**, 517 (1991).
[15] Ph. Mounaix *et al.*, Phys. Fluids B **5**, 3304 (1993).
[16] G. Bonnaud, D. Pesme, and R. Pellat, Phys. Fluids B **2**, 1618 (1990).
[17] T. Kolber, W. Rozmus, and V. T. Tikhonchuk, Phys. Fluids B **5**, 138 (1993).
[18] H. A. Baldis *et al.*, Phys. Fluids B **5**, 3319 (1993).
[19] S. D. Baton *et al.*, Phys. Rev. E **49**, 3602 (1994).